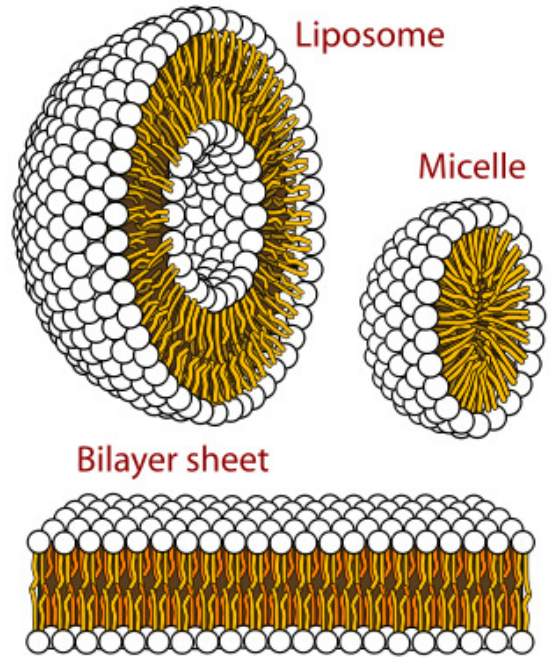
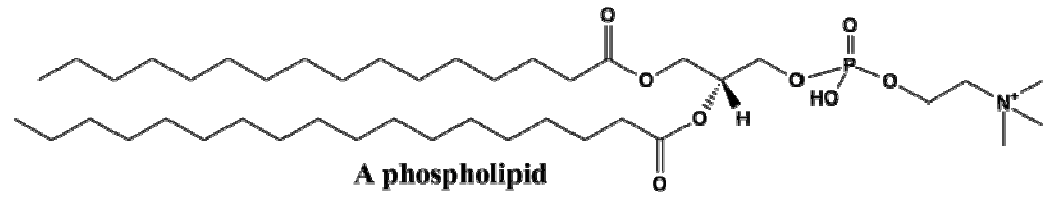
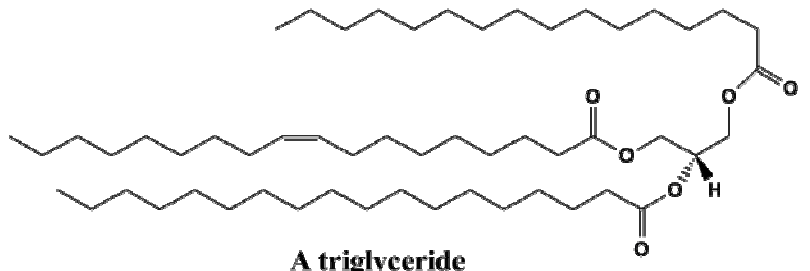
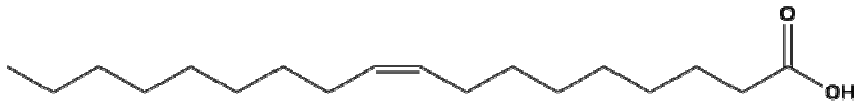
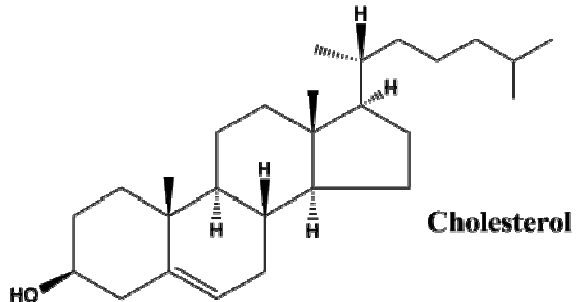


Lipids

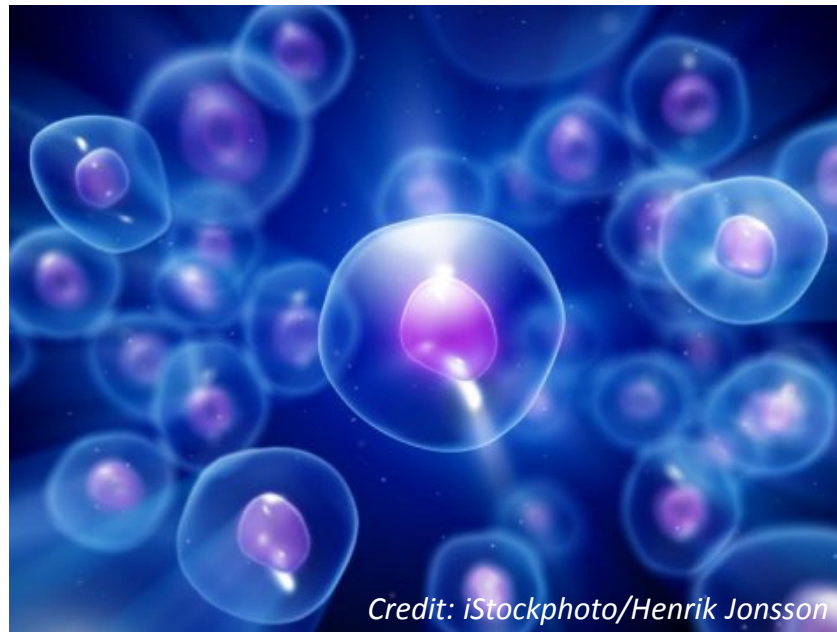


By Mariana Ruiz Villarreal

By Lmaps

Encapsulation – essential for life

Evolving chemical systems require compartments for Darwinian evolution – to compete, to store information and to concentrate reactants/metabolites



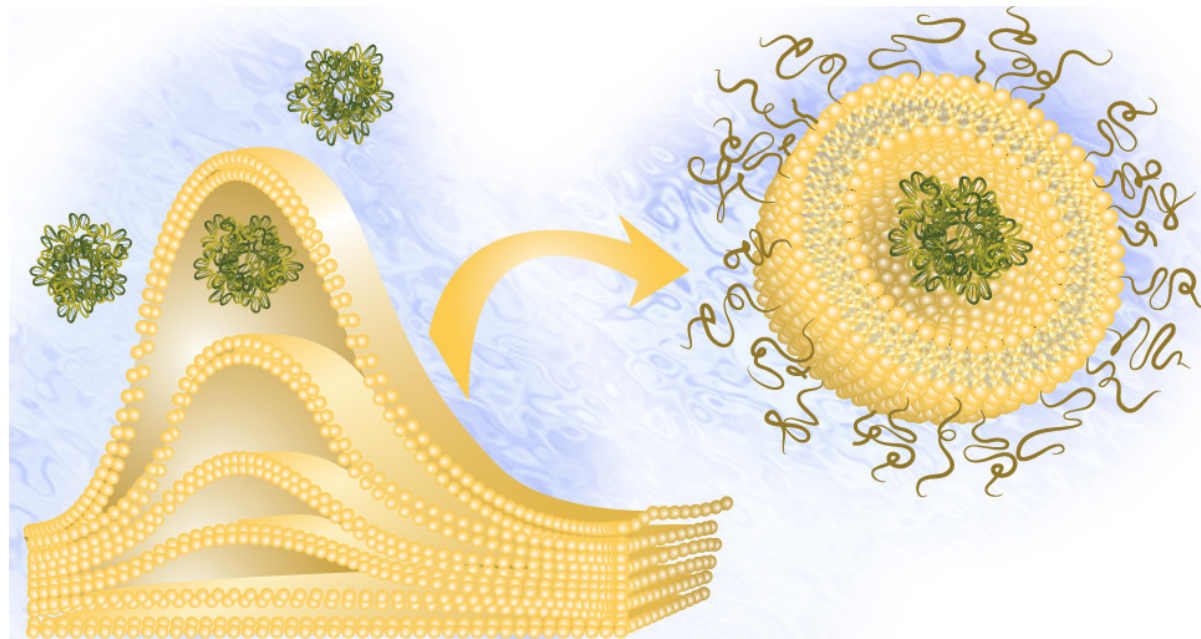
Credit: iStockphoto/Henrik Jonsson

Encapsulation into membranes is considered an early stage in prebiotic chemical evolution and essential requirement for the emergence of life

Encapsulation – essential for life

Formation of membranes is most easy to explain among major cellular components of the prebiotic Earth.

Many amphiphilic organic compounds spontaneously form vesicles in water at sufficiently high concentrations

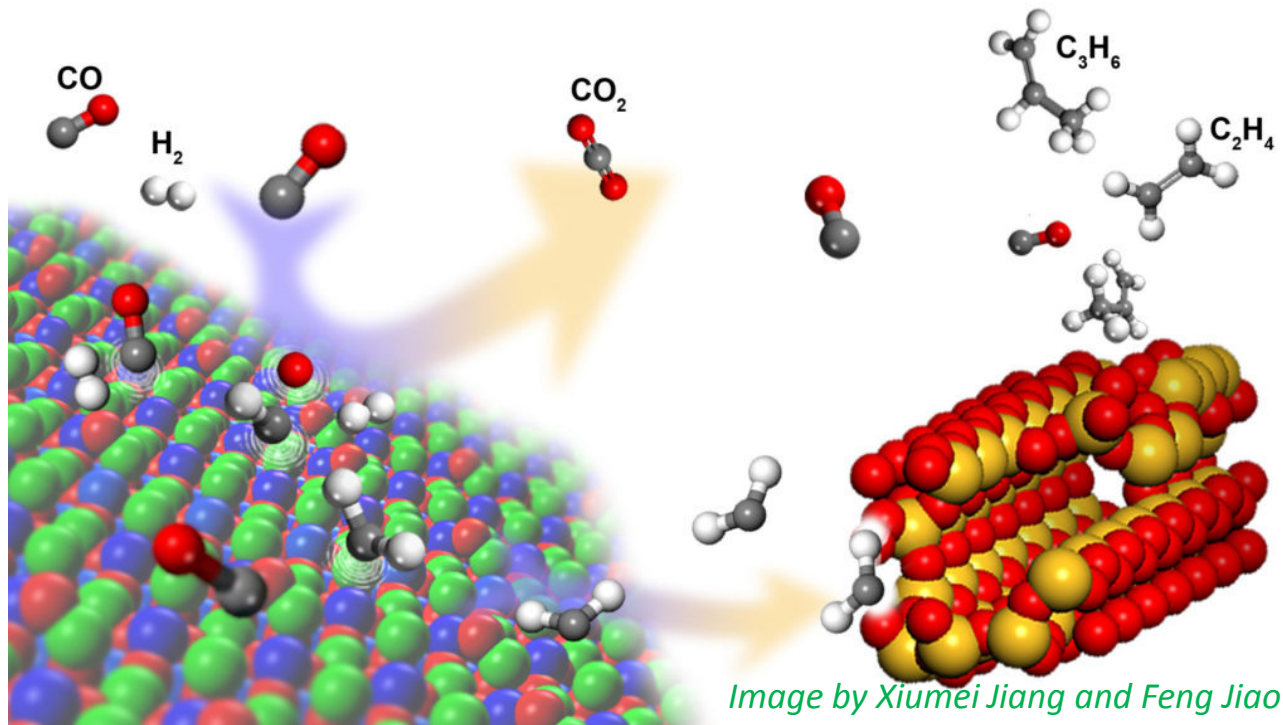


Levine, R.M., Pearce, T.R., Adil, M., Kokkoli, E. Langmuir, 2013, 29 (29): 9208–9215.

The vesicle will encapsulate an aqueous solution inside a thin layer of organic material

Fischer-Tropsch synthesis

Long hydrocarbon chains from CO + H₂ in presence of metal catalysts and high pressure, fatty acids and alcohols are minor by-products



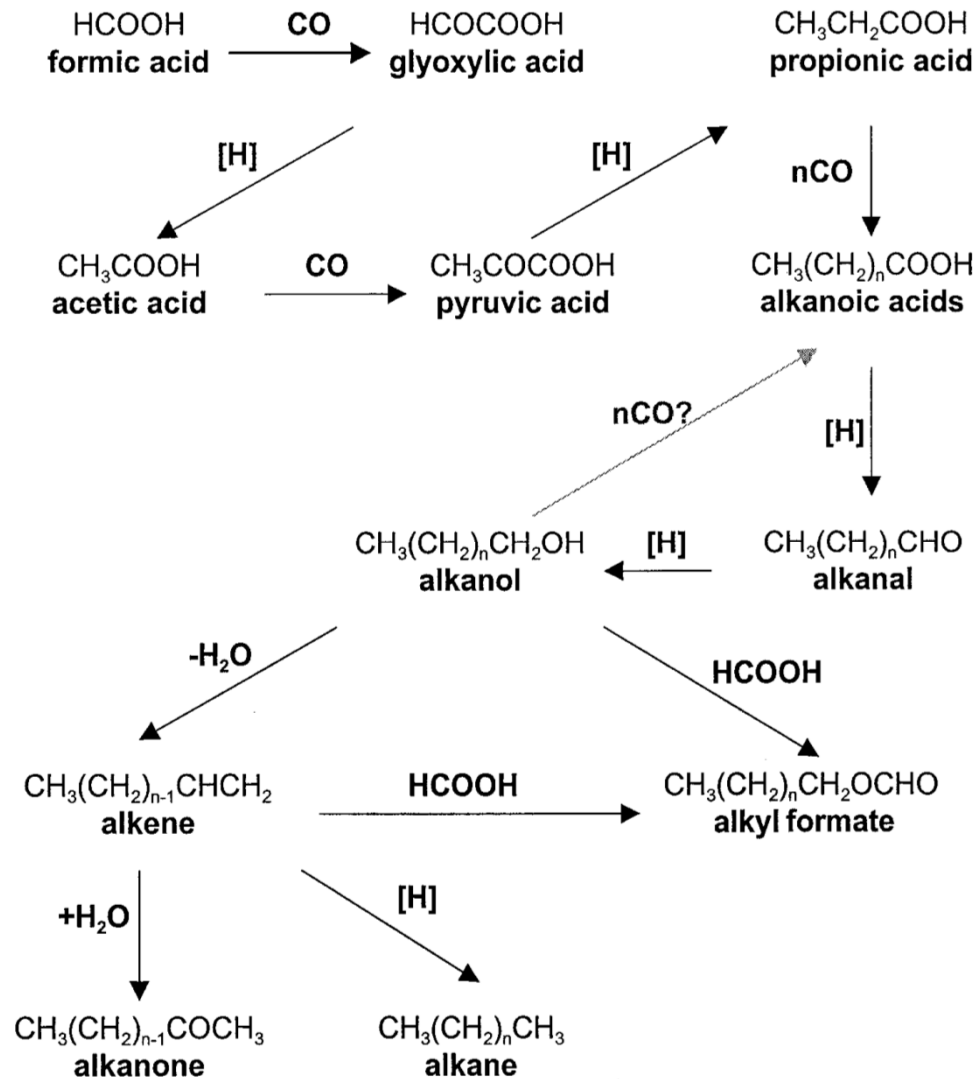
The mixture of D₂ and CO over meteoritic iron or iron ore produced alkanes and n-fatty acids

Oro, J. et al. Geochim. Cosmochim. Acta **1976**, 40, 915-924.

Fischer-Tropsch synthesis

Main reactions	
1. Paraffins	$(2n+1)H_2+nCO \rightarrow C_nH_{2n+2} +nH_2O$
2. Olefins	$2nH_2+nCO \rightarrow C_nH_{2n} +nH_2O$
Side reactions	
3. Water-Gas-Shift (WGS)	$CO+H_2O \leftrightarrow CO_2+H_2$
4. Carbide formation	$yC + xM \leftrightarrow M_xC_y$
5. Alcohols	$2nH_2+nCO \rightarrow C_nH_{2n}+2O +(n-1)H_2O$
6. Boudouard reaction	$2CO \rightarrow C +CO_2$
7. Catalyst reduction and oxidation	$M_xO_y + yH_2 \leftrightarrow xM + yH_2O$
	$M_xO_y + yCO \leftrightarrow xM + yCO_2$
8. Coking	$H_2 + CO \rightarrow C + H_2O$

Hydrothermal Fischer-Tropsch synthesis



Formic or oxalic acid heated in water at 150-250⁰C (stainless steel reactor) yielded a mixture of C₁₂-C₃₃ lipids

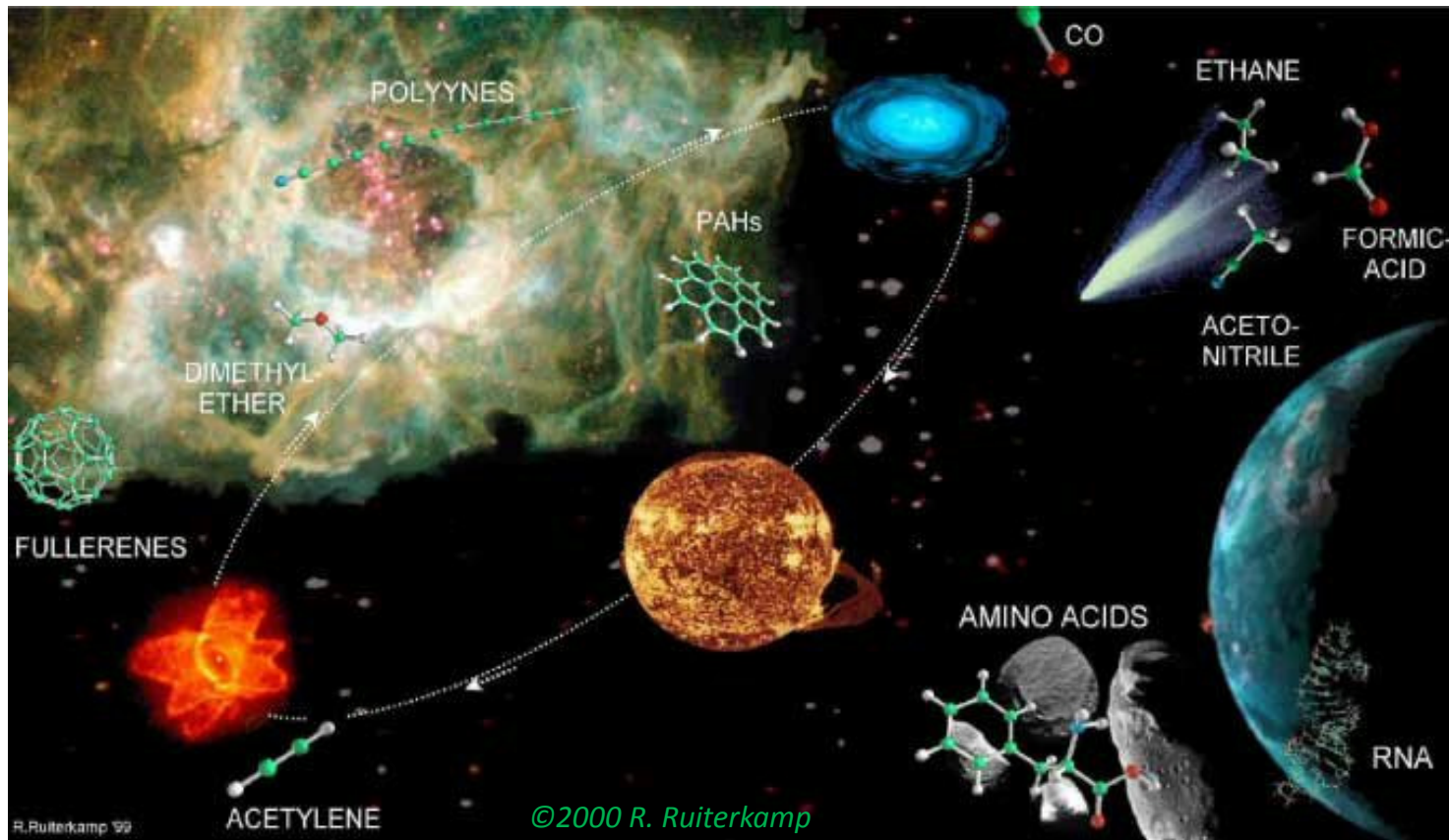
Rushdi, A., Simoneit B. Origins Life Evol. Biospheres **2001**, 31, 103-118

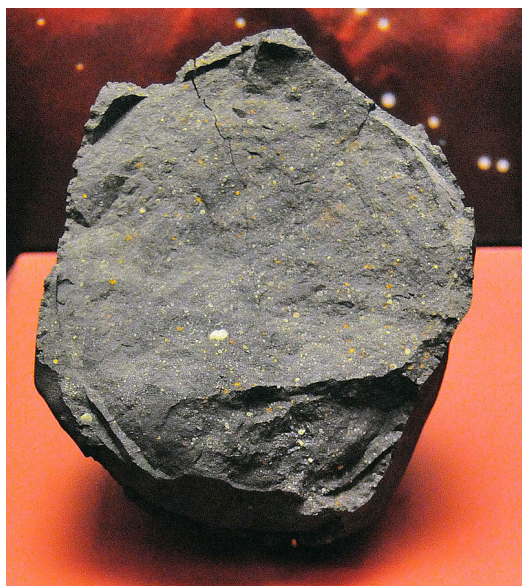
When CO, H₂ and NH₃ are allowed to react at 200-700⁰C in presence of Ni, Al, or clay catalysts, aminoacids are detected:

glycine, alanine, sarcosine, aspartic acid, glutamic acid, arginine, histidine, lysine and ornithine

Yoshino, D.; Hayatsu, R.; Anders, E. Geochim. Cosmochim. Acta **1971**, 35, 927-938

Extraterrestrial origin of biomolecules





Murchison meteorite
chondrite

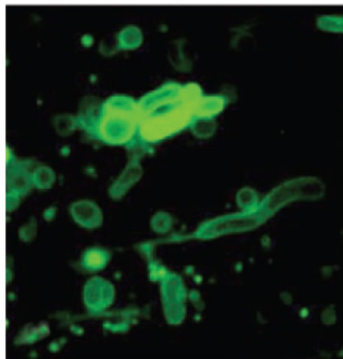
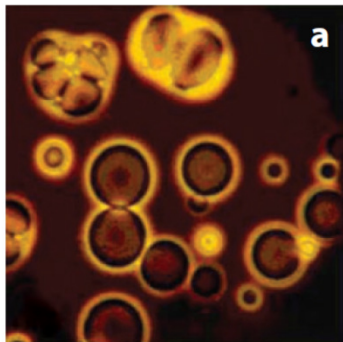
Table 1. Soluble Organic Compounds in the Murchison Meteorite^a

class of compounds	parts per million	<i>n</i> ^b
aliphatic hydrocarbons	>35	140
aromatic hydrocarbons	15–28	87
polar hydrocarbons	<120	10 ^d
carboxylic acids	>300	48 ^d
amino acids	60	75 ^d
imino acids	nd ^c	10
hydroxy acids	15	7
dicarboxylic acids	>30	17 ^d
dicarboximides	>50	2
pyridinecarboxylic acids	>7	7
sulfonic acids	67	4
phosphonic acids	2	4
<i>N</i> -heterocycles	7	31
amines	13	20 ^d
amides	nd ^c	27
polyols	30	19

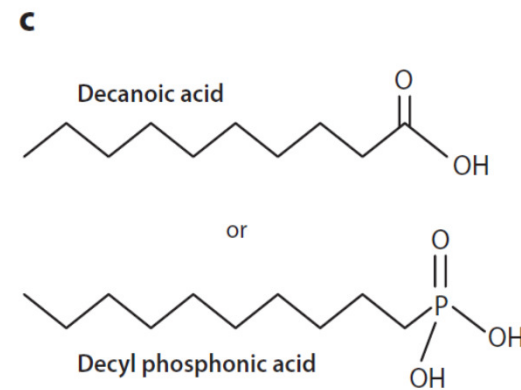
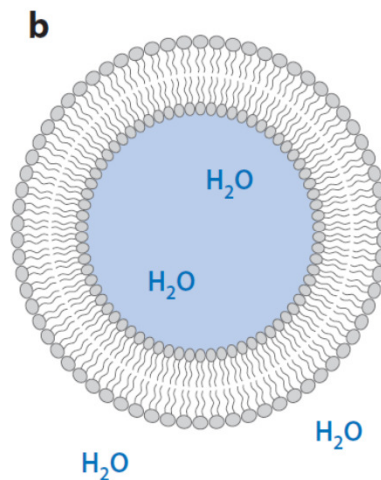
Encapsulation – essential for life

Fatty acids have been found in meteorites – plausible prebiotic synthesis pathways existed in the early Solar System

Meteorite extracts



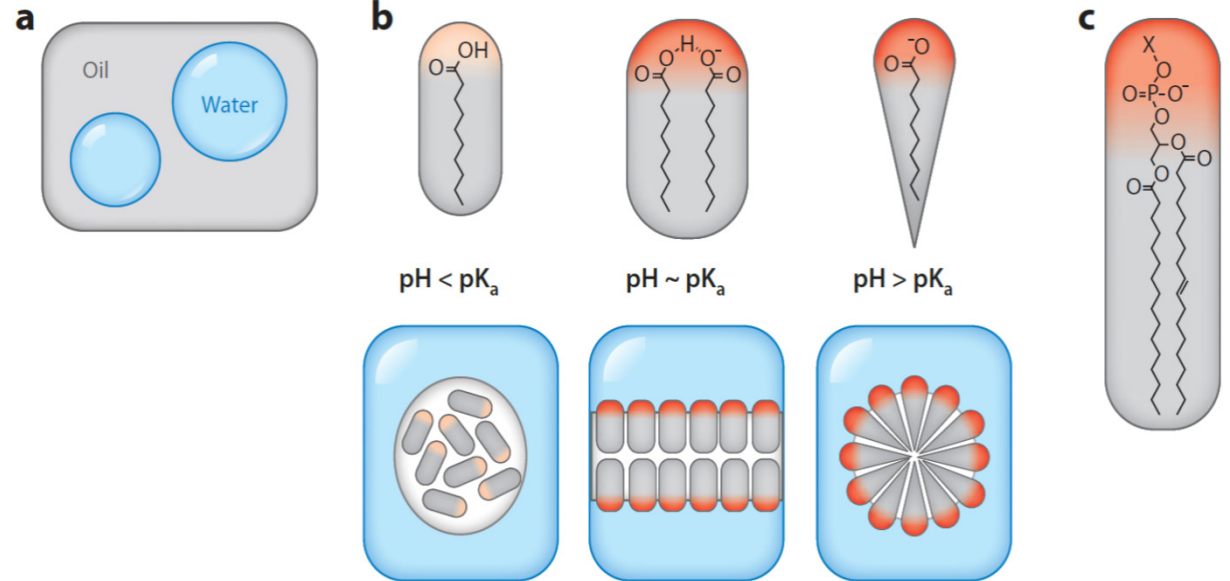
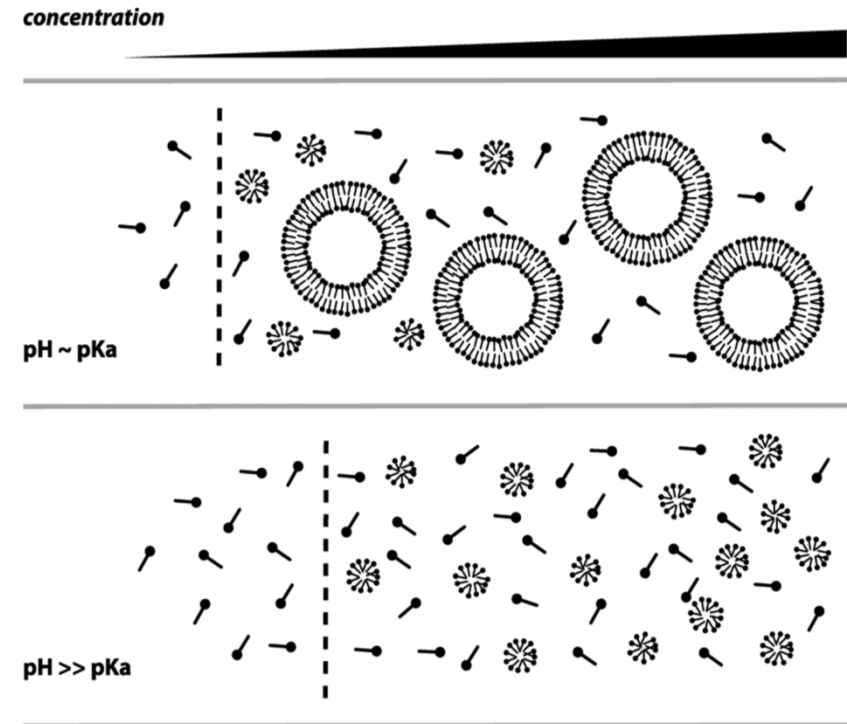
Decanoic acid



Extracts of meteorites containing these compounds spontaneously form vesicles when hydrated

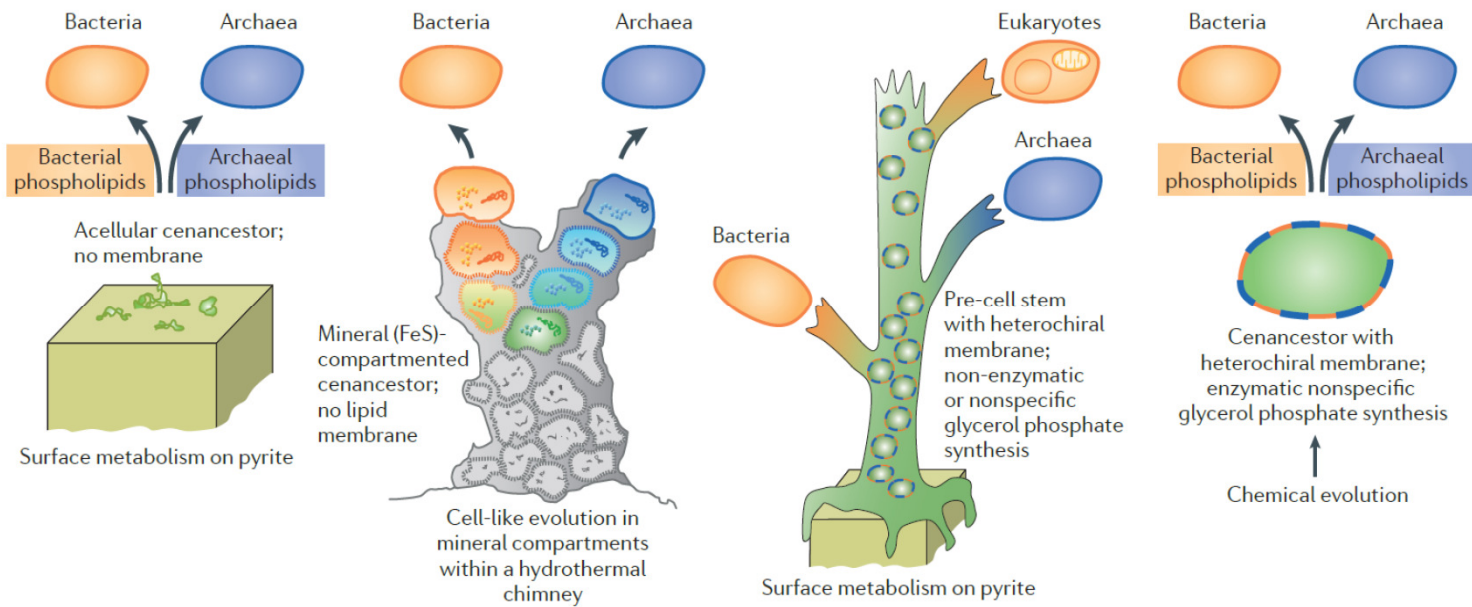
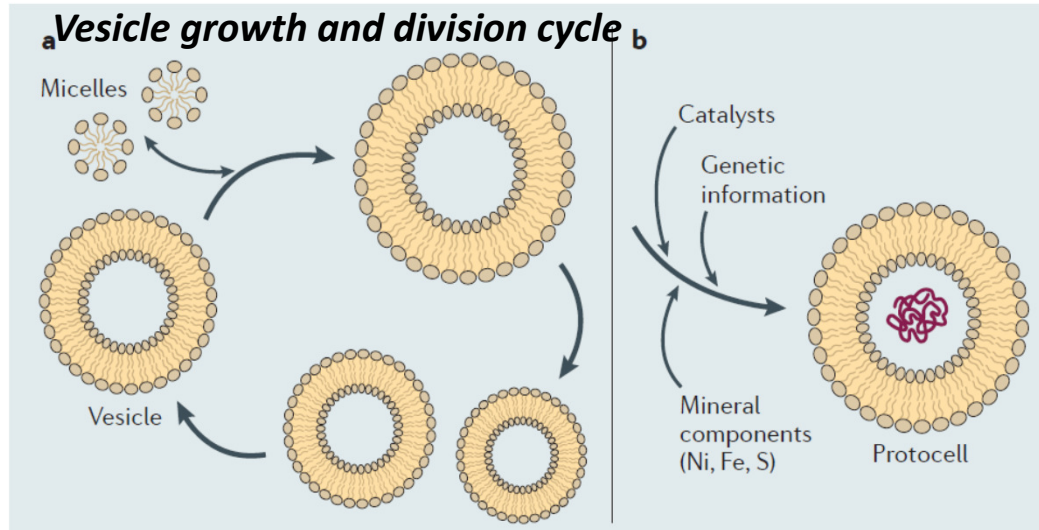
Spontaneous generation of lipid vesicles

The first protocell membranes may have assembled from fatty acids and related single-chain lipids available in the prebiotic environment.



At different concentrations, fatty acids can partition between several different phases, including soluble monomers, micelles, and lamellar vesicles, with higher concentrations favoring larger vesicle aggregates.

Transition: Micelles-Vesicles-Protocells





Jack Szostak

(* November 9, 1952) - Canadian American biologist of Polish British descent,

Nobel Prize laureate 2009 for Physiology and Medicine, for the discovery of how chromosomes are protected by telomeres; Professor of Genetics at Harvard Medical School.

Szostak has made significant contributions to the field of genetics. His achievement helped scientists to map the location of genes in mammals and to develop techniques for manipulating genes.

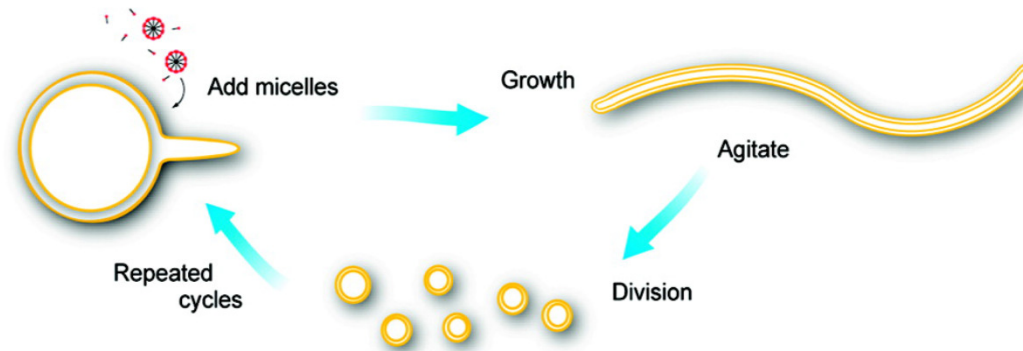
His research findings in this area are also instrumental to the Human Genome Project.

By Markus Pössel (Mapos)

In the early 90s his laboratory shifted its research direction and focused on studying **RNA enzymes**, which had been recently discovered by Cech and Altman. He developed the technique of **in vitro evolution of RNA** (also developed independently by Gerald Joyce) which enables the discovery of RNAs with desired functions through successive cycles of selection, amplification and mutation. He isolated the first **aptamer** (term he used for the first time). He isolated **RNA enzymes with RNA ligase activity** directly from random sequence (project of David Bartel).

Currently his lab focuses on the challenges of understanding the **origin of life** on Earth, and the construction of **artificial cellular life** in the laboratory

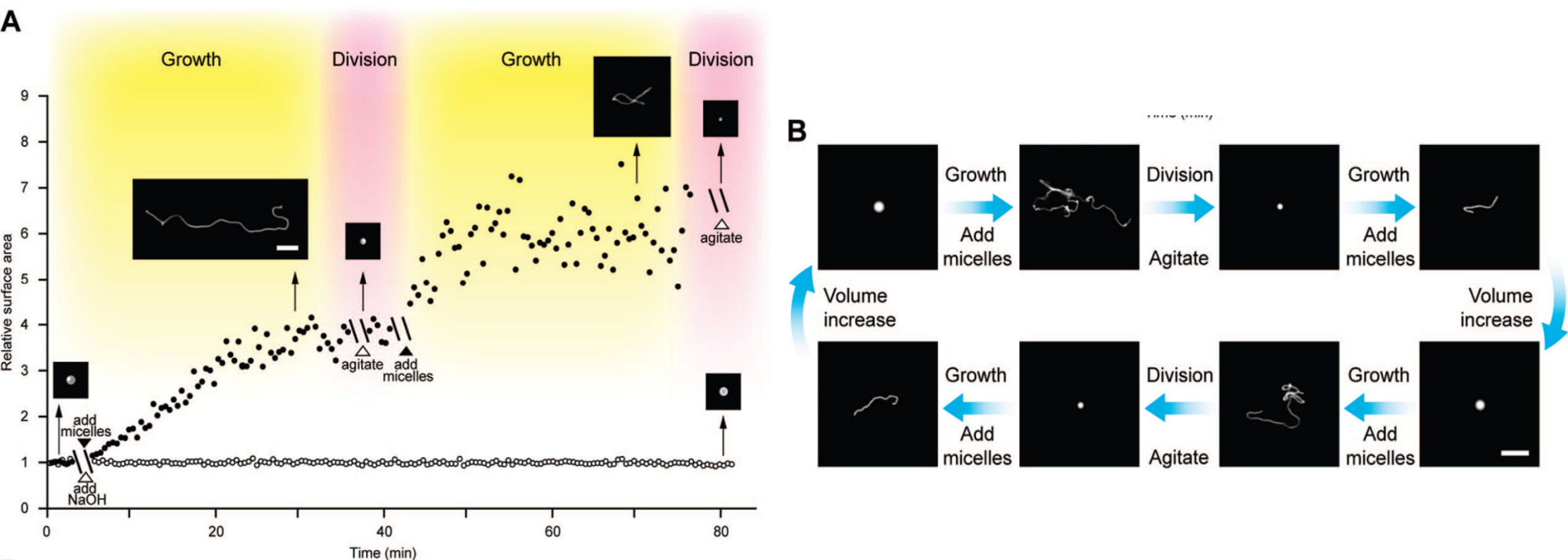
Coupled growth and division of model protocell membranes



The growth of large multilamellar fatty acid vesicles fed with fatty acid micelles, in a solution where solute permeation across the membranes is slow, results in the transformation of initially spherical vesicles into long thread-like vesicles, a process driven by the transient imbalance between surface area and volume growth. Modest shear forces are then sufficient to cause the thread-like vesicles to divide into multiple daughter vesicles without loss of internal contents.

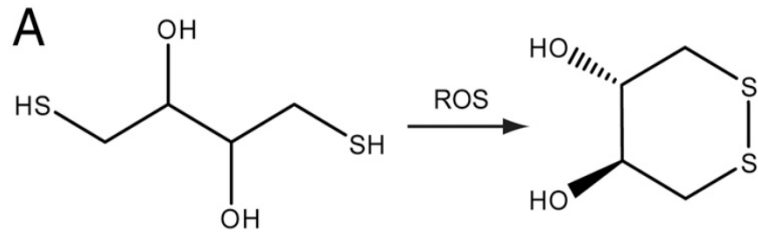


Coupled growth and division of model protocell membranes



Cycles of vesicle growth and division. (A) Relative surface area after two cycles of addition of 5 equiv of oleate micelles (solid circles) or 5 equiv of NaOH (open circles) to oleate vesicles, each followed by agitation. Inset micrographs show vesicle shapes at indicated times. Scale bar, 10 μm . (B) Vesicle shapes during cycles of growth and division in a model prebiotic buffer (0.2 M Na-glycine, pH 8.5, ~ 1 mM initial oleic acid, vesicles contain 10 mM HPTS for fluorescence imaging). Scale bar, 20 μm .

Ting F. Zhu, and Jack W. Szostak *J. Am. Chem. Soc.*, **2009**, 131 (15), 5705-5713



Photochemically driven protocell division

The illumination of filamentous fatty acid vesicles rapidly induces pearling and subsequent division in the presence of thiols.

Photochemically generated reactive oxygen species oxidize thiols to disulfide-containing compounds that associate with fatty acid membranes, inducing a change in surface tension and causing pearling and subsequent division.

Alternative route for the emergence of early self-replicating cell-like structures, particularly in thiol-rich surface environments.

The subsequent evolution of cellular metabolic processes controlling the thiol:disulfide redox state would have enabled autonomous cellular control of the timing of cell division, a major step in the origin of cellular life.

Oleate vesicle pearling and division.

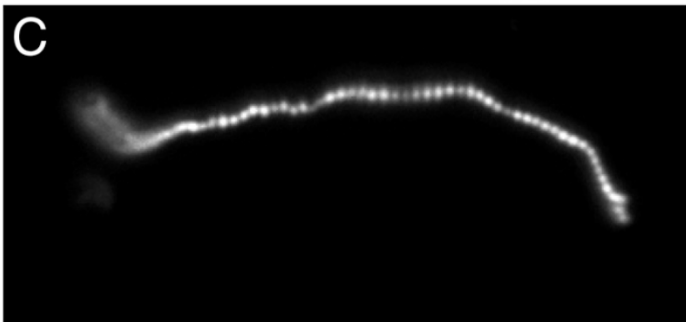
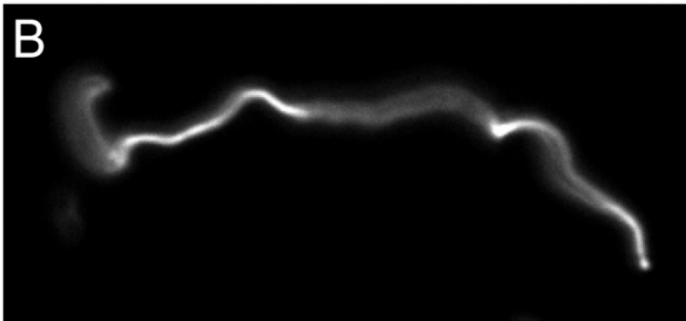
A. Radical-mediated oxidation of DTT.

B. An oleate vesicle (containing 2 mM HPTS, in 0.2 M Na-glycinamide, pH 8.5, 10 mM DTT) 30 min after the addition of five equivalents of oleate micelles.

C. and D. Under intense illumination (for 2 s and 12 s, respectively), the long thread-like vesicle went through pearling and division

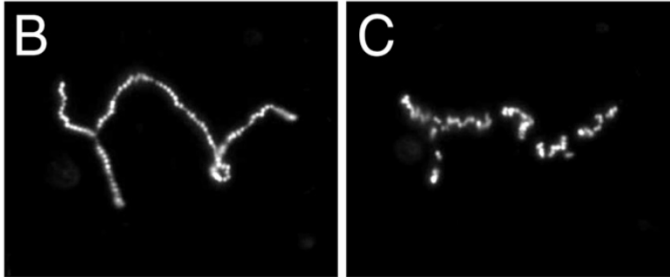
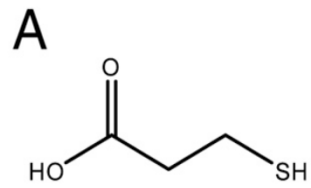
Scale bar, 10 μ m.

T. F. Zhu, K. Adamala, N. Zhang, J. W. Szostak *PNAS*, 2012, doi:10.1073/pnas.1203212109



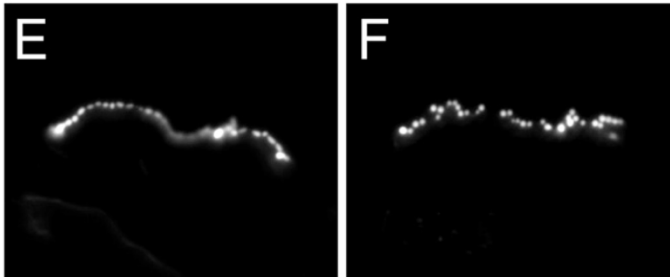
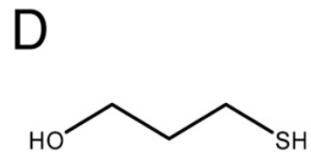
Photochemically driven protocell division

Oleate vesicle pearling and division with various thiols in the solution.



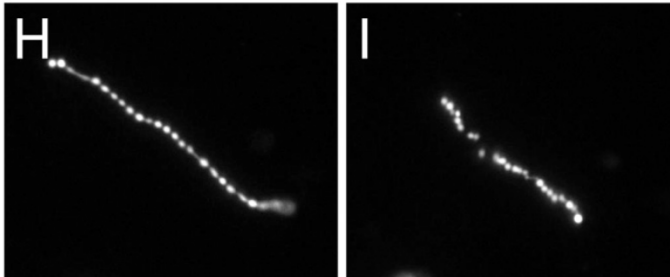
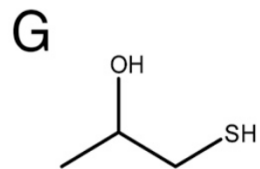
(A) 3-mercaptopropionic acid.

(B and C) An oleate vesicle (containing 2 mM HPTS, in 0.2 M Na-bicine, pH 8.5, 10 mM 3-mercaptopropionic acid, 30 min after the addition of five equivalents of oleatemicelles) went through pearling and division under intense illumination (for 3 s and 15 s, respectively).



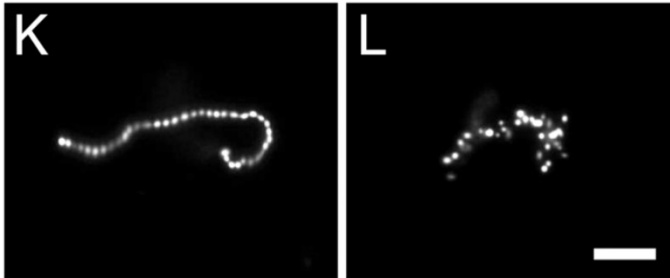
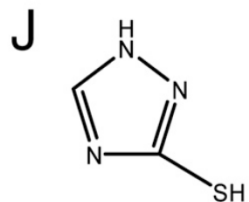
(D) 3-mercaptopropanol.

(E and F) An oleate vesicle as above but in 50 mM 3-mercaptopropanol, went through pearling and division under intense illumination (for 2 s and 10 s, respectively).



(G) 1-mercaptopropan-2-ol.

(H and I) An oleate vesicle as above but in 50 mM 1-mercaptopropan-2-ol went through pearling and division under intense illumination (for 2 s and 9 s, respectively).

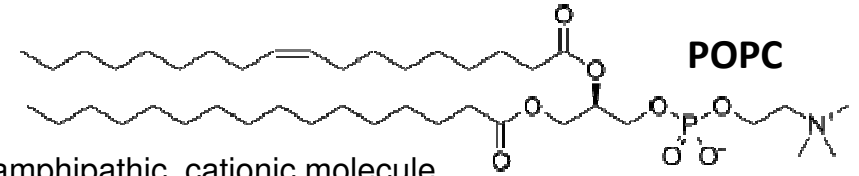
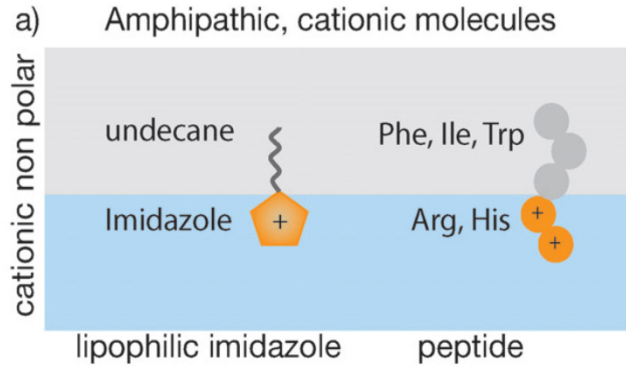


(J) 3-mercaptopropan-1,2,4-triazole.

(K and L) An oleate vesicle as above but in 50 mM 3-mercaptopropan-1,2,4-triazole went through pearling and division under intense illumination (for 3 s and 13 s, respectively).

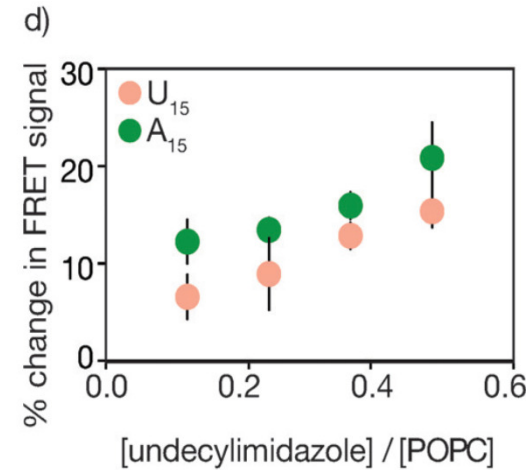
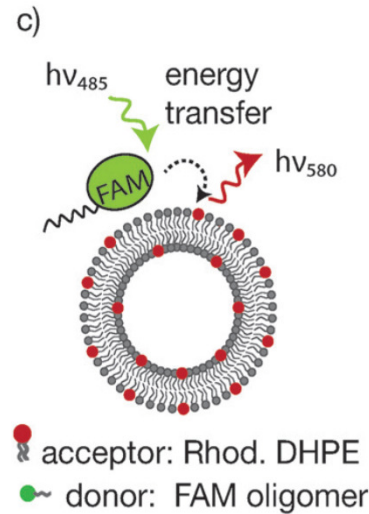
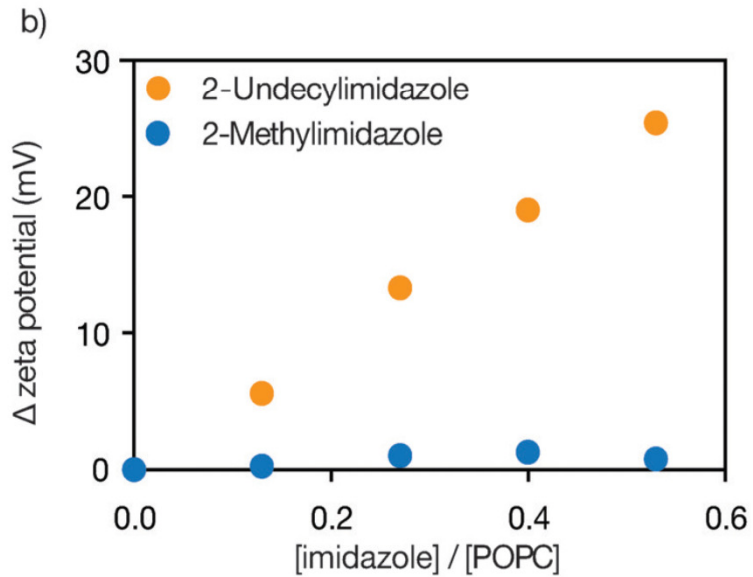
Scale bar, 20 μm .

Noncovalent nucleotide association with membranes

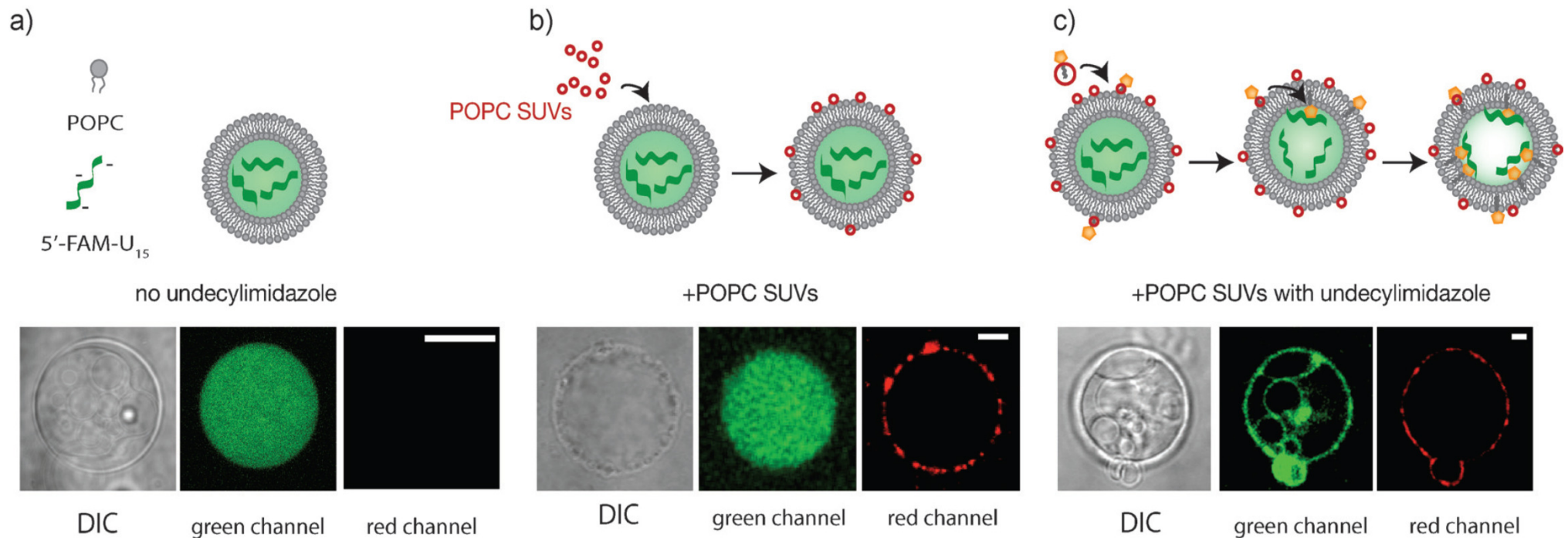


RNA localization with a model amphipathic, cationic molecule

- Design of RNA-localizing molecules that include both nonpolar and cationic regions.
- The change in zeta potential
- Schematic of the FRET assay used to assess RNA localization to vesicle membranes
- RNA (5'-FAM-U₁₅ and 5'-FAM-A₁₅) shows increasing localization to POPC membranes that contain increased amounts of undecylimidazole.



Noncovalent nucleotide association with membranes



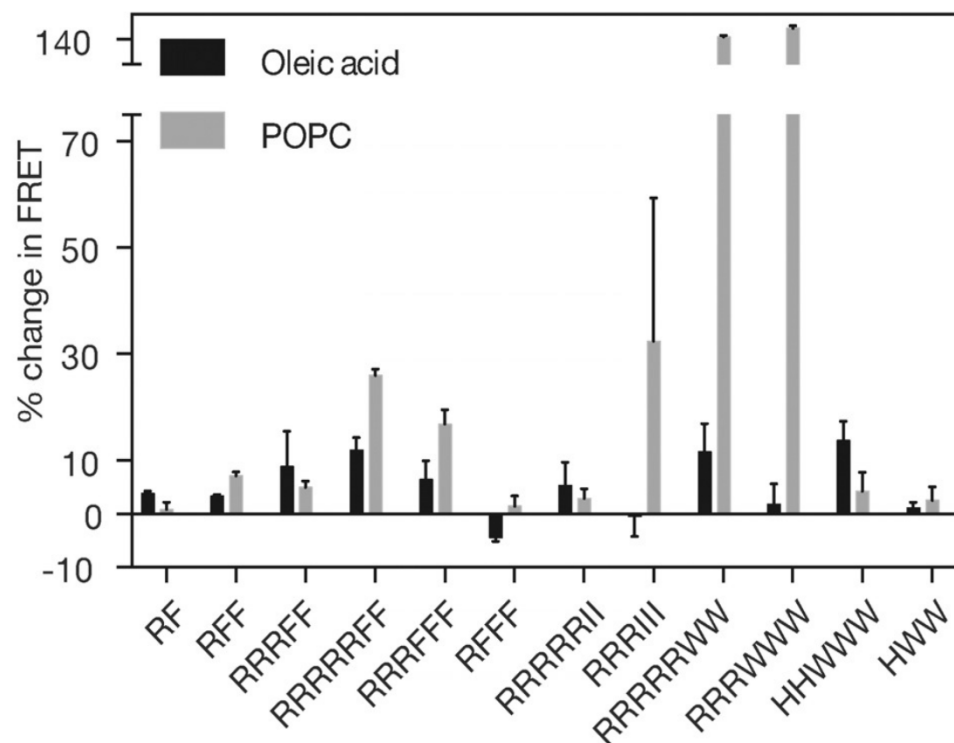
Microscopy of encapsulated RNA localization to POPC membranes with 2-undecylimidazole. Confocal images of 5'-FAM-U₁₅ RNA (green) association with giant POPC vesicles membranes in the presence of 2-undecylimidazole. Differential interference contrast (DIC) microscopy images are shown for each vesicle.

- RNA appears uniformly distributed in the interior of POPC GUVs.
- The addition of SUVs containing a rhodamine-labeled lipid (red) leads to SUV aggregation and association with the giant vesicle membranes, but RNA (green) remains uniformly encapsulated in the vesicle interior.
- The addition of SUVs containing a rhodamine-labeled lipid (red) and 40 mol% 2-undecylimidazole leads to SUV association with vesicle membranes and RNA (green) localizes to the vesicle surface. The scale bar is 20 nm.

SUV – small unilamellar vesicle **GUV – giant unilamellar vesicle (5-25 μm)**

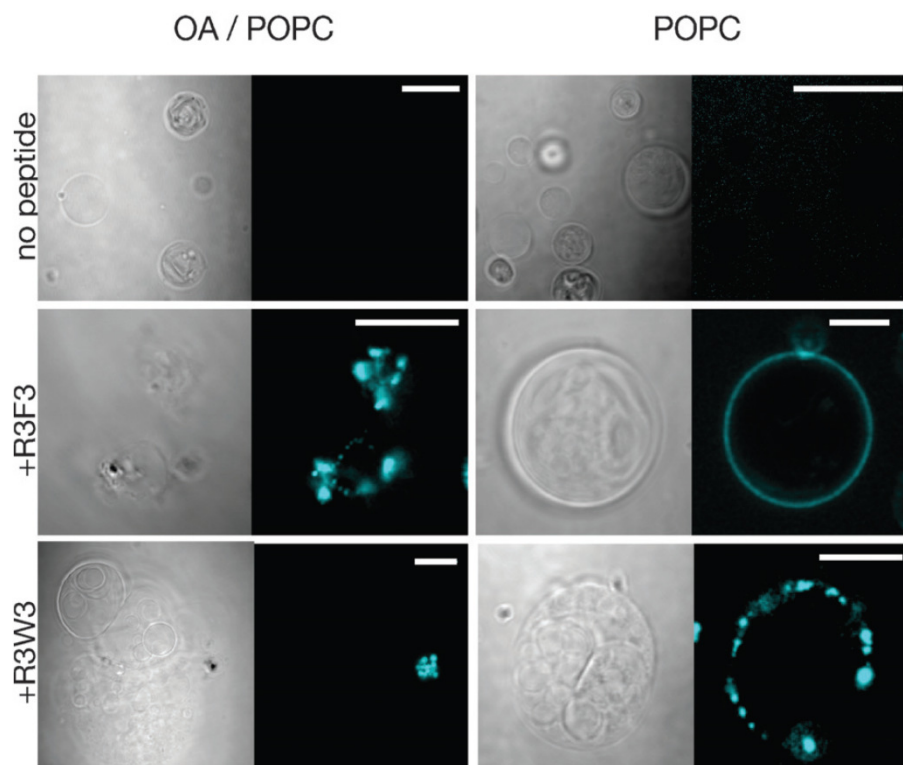
Neha P. Kamat, Sylvia Tobe, Ian T. Hill, and Jack W. Szostak *Angew. Chem. Int. Ed.* **2015**, *54*, 11735–11739

Noncovalent nucleotide association with membranes

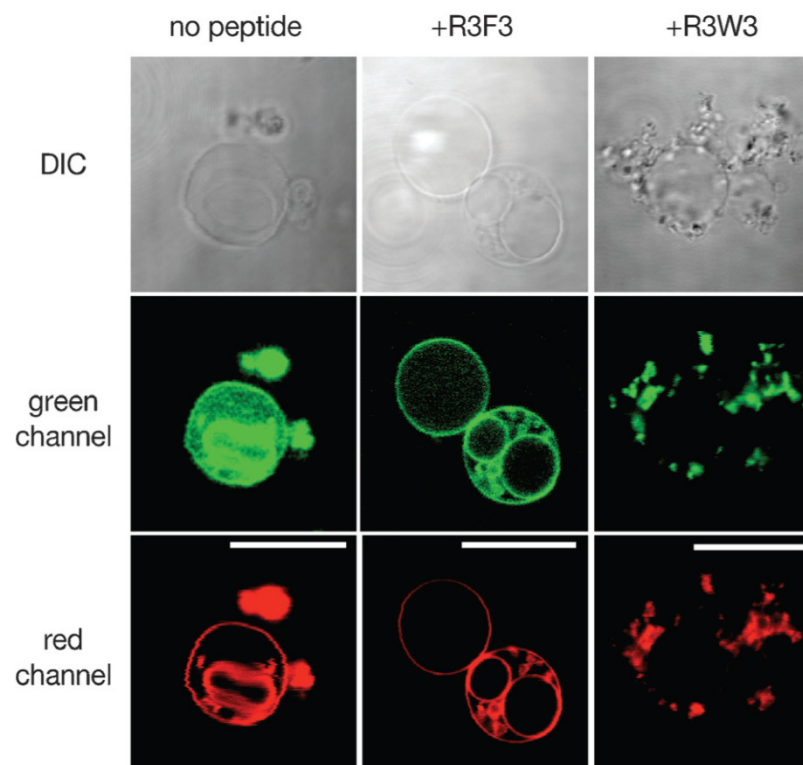


Peptide-induced RNA–membrane association. A FRET assay reports RNA localization (5'-FAM-U₁₅) to POPC and oleic acid membranes (7.5 μ m) 10 h after the addition of 1 μ M of various peptides to the vesicle solution at pH 8. Data is reported as a percentage change from control samples that lack peptide. $n=4$, error bars represent the standard error of the mean.

Noncovalent nucleotide association with membranes



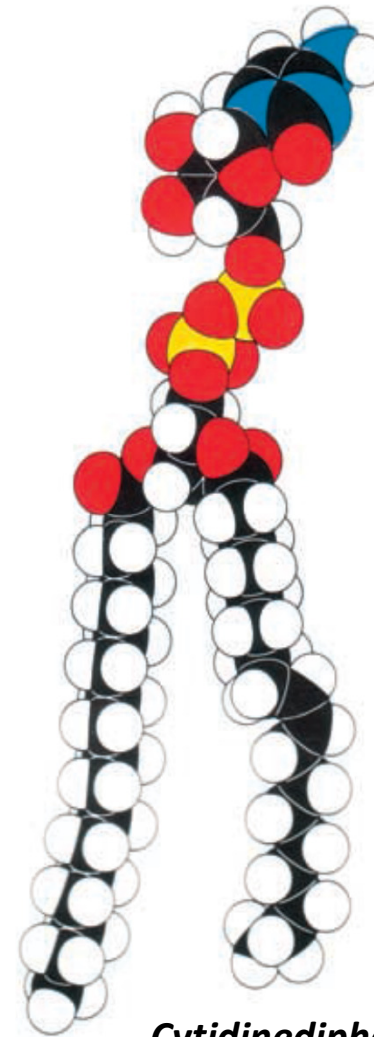
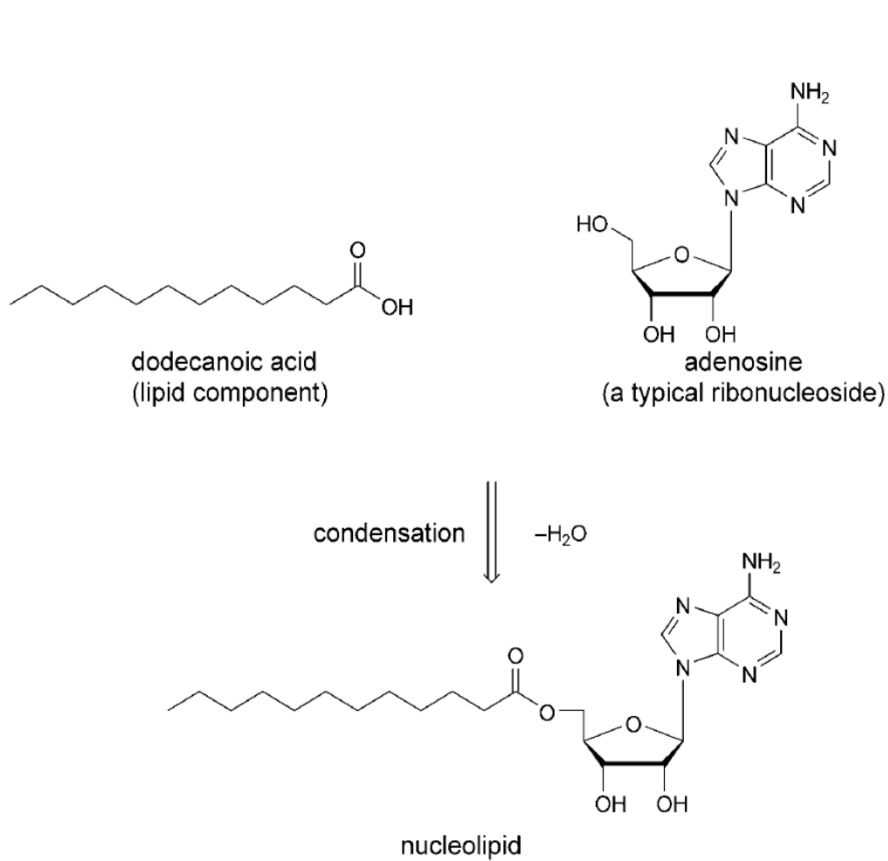
Microscopy of peptide-induced RNA–membrane association. Confocal images show RNA localization (5'-AlexaFluor647-labeled 15-mer, cyan) to the outside of oleic acid/POPC (90%/10%) and pure POPC membranes in the presence of R3F3 and R3W3 peptides. Control samples had no peptide added. For each image, the left panel shows the DIC image and the right panel shows AlexaFluor647 fluorescence. The scale bar is 20 nm.



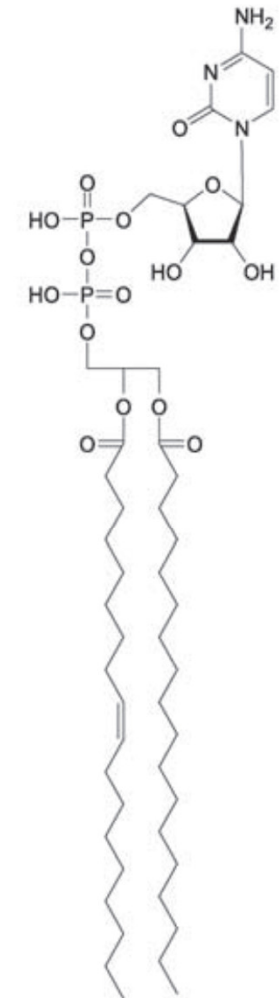
Microscopy of encapsulated RNA localization to POPC membranes with peptides. Confocal images show that RNA (5'-FAMU₁₅, green) encapsulated in POPC vesicles (containing a rhodamine-labeled lipid, red) becomes localized to the membrane of certain vesicles after an overnight incubation with R3F3 and R3W3 peptides. The scale bar is 20 nm.

Neha P. Kamat, Sylvia Tobe, Ian T. Hill, and Jack W. Szostak *Angew. Chem. Int. Ed.* **2015**, *54*, 11735–11739

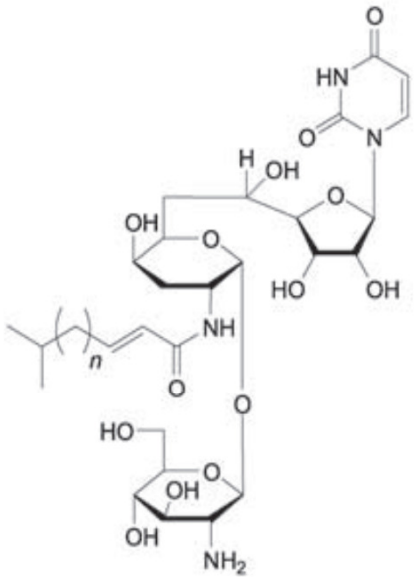
Nucleolipids – a replication mechanism for genetic information?



Cytidinediphosphatediacylglycerol

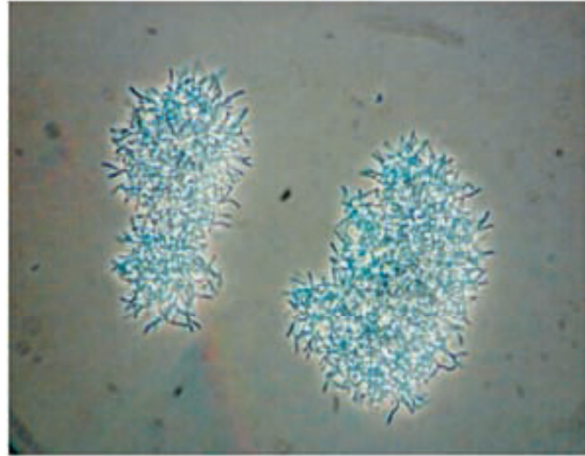


Antibiotic nucleolipids



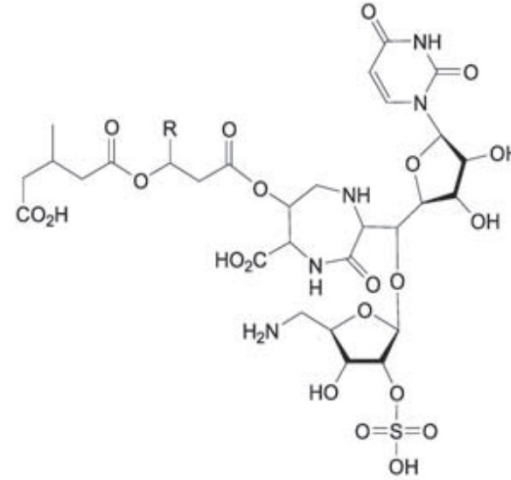
- 2 Tunicamycin A $n = 9$
- 3 Tunicamycin B $n = 10$
- 4 Tunicamycin C $n = 8$
- 5 Tunicamycin D $n = 11$

from *Streptomyces lysosuperficus*

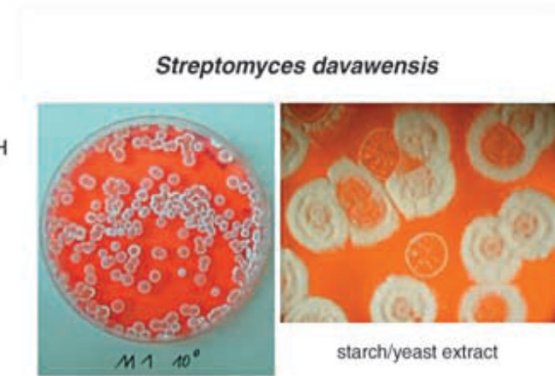


Streptomyces lysosuperficus

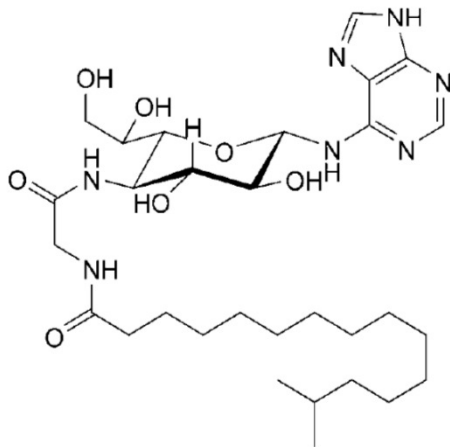
Inhibit peptidoglycan synthesis



- 6 Liposidomycin B $R = \text{Me}_2\text{CH}(\text{CH}_2)_8$
- 7 Liposidomycin C $R = \text{Me}(\text{CH}_2)_{10}$

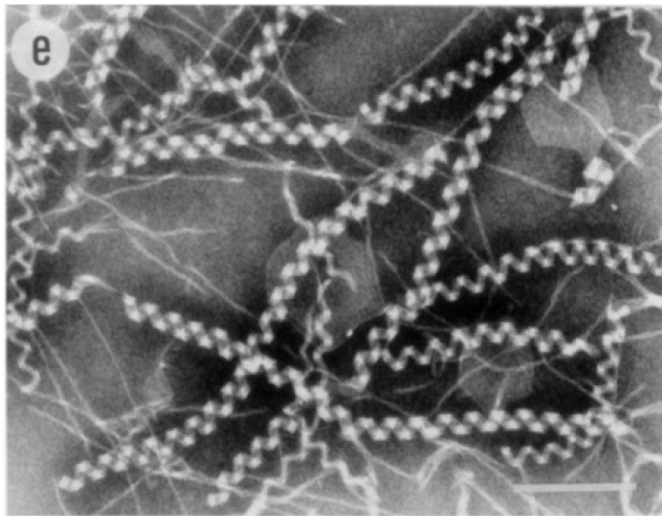
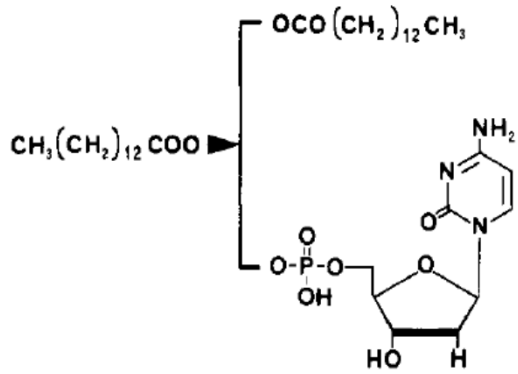


Streptomyces davawensis

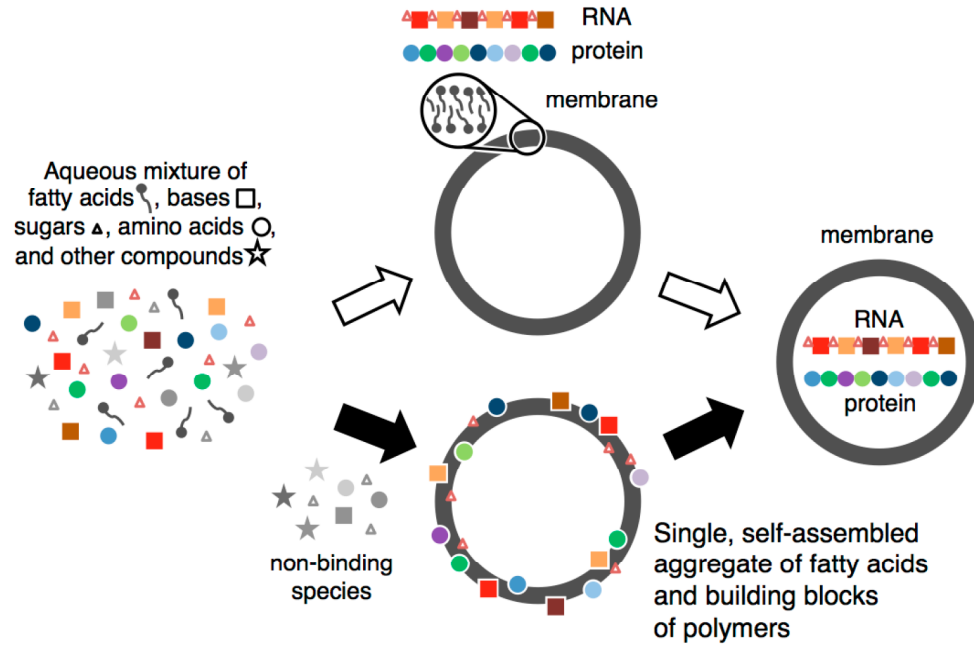


Septacidine (8)
from *Streptomyces fimbriatus*

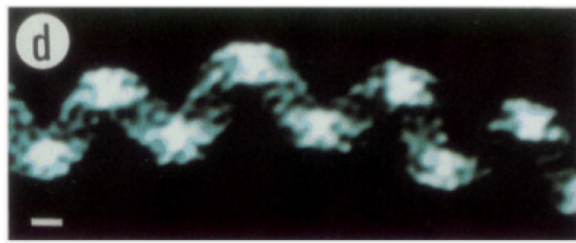
Nucleolipids – a replication mechanism for genetic information?



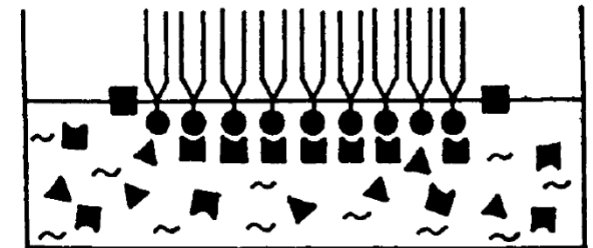
Scalebar: 200 nm



Black, R. A.; Blosser, M. C. *Life* **2016**, *6*(3), 33; doi:10.3390/life6030033



Scalebar: 10 nm



\blacksquare = adenine (complementary)
 \blacktriangle = thymine (noncomplementary)

Yanagawa, H. et al. *J. Am. Chem. Soc.* **1989**, *111*, 4567-4570

Rosemeyer, H. *Chem. Biodiversity* **2005**, *2*, 977

Phosphates



Source: Google Images

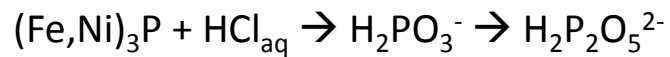


Wikimedia , Butcherbird

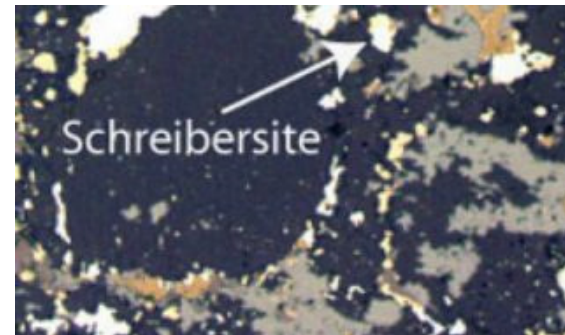
slice of the Gebel Kamil Meteorite with schreibersite rimmed by kamacite

Schreibersite is generally a rare iron-nickel phosphide mineral, $(\text{Fe,Ni})_3\text{P}$, though common in iron-nickel meteorites

Acidic schreibersite corrosion under anaerobic conditions (10% aq. HCl/N_2) \rightarrow soluble forms of phosphorus



T. P. Kee *et al.* *Geochimica et Cosmochimica Acta*. **2013** 109, 90-112



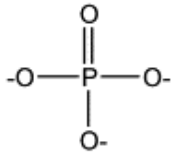
Virginia Smith, UA Lunar & Planetary Laboratory



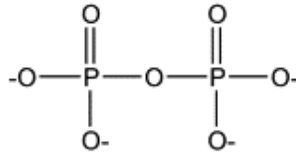
Image of schreibersite grain present in a thin-section of the enstatite meteorite, KLE 98300.

Phosphates

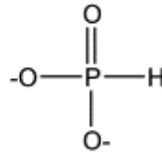
I. Orthophosphate



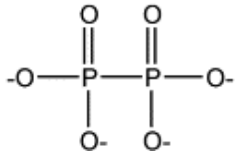
II. Pyrophosphate



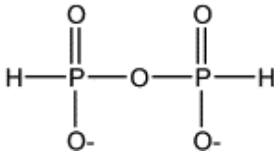
III. Phosphite



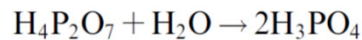
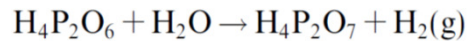
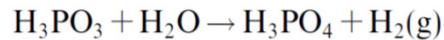
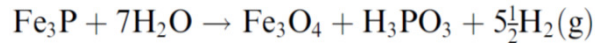
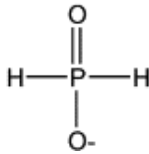
IV. Hypophosphate



V. Diphosphate

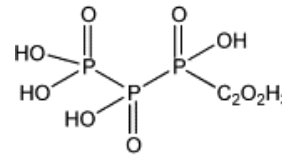
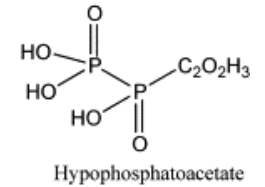
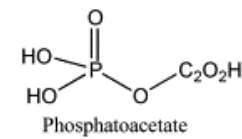
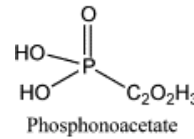
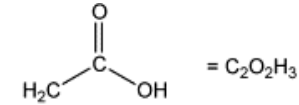


VI. Hypophosphite

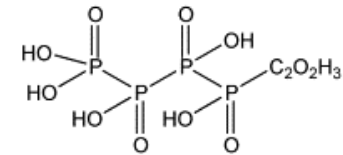


Radical pathway of the corrosion is suggested.
In presence of simple organic molecules (e.g. acetic acid)
organophosphorous compounds are detected

I. Acetyl-P compounds



Tri-P-acetate

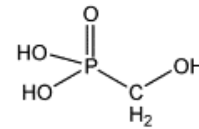


Quad-P-acetate

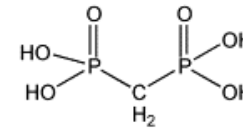
Etc.

Penta-P-Acetate

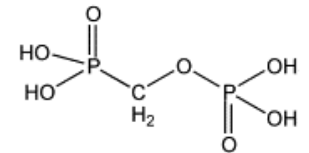
II. Methyl-P Compounds



Phosphonomethanol

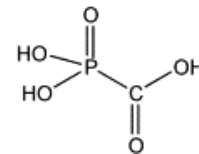


Dimethylphosphite

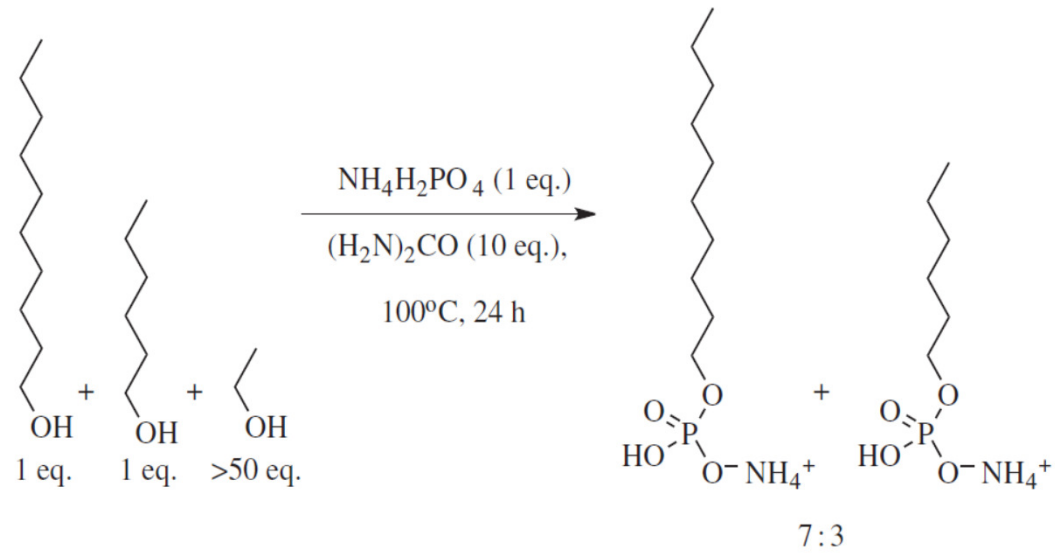


Phosphonomethylphosphate

III. Phosphonoformate



Phospholipids



Lipids - summary

Many amphiphilic organic compounds spontaneously form vesicles in water at sufficiently high concentrations

Current phospholipid membranes likely evolved late. Protocells probably encapsulated by fatty acids, fatty alcohols, prenyl oligomers, or phosphorylated alcohols

Nucleolipids are proposed as intermediates in templated oligonucleotide replication

Phosphorus was accessible upon corrosion of meteorite materials and could be incorporated into lipids

The origin of small reactive intermediates



vivianite

Schreibersite (Fe,Ni)₃P, from iron-nickel meteorites: source of phosphorus, iron and nickel

Under more neutral conditions phosphates recombine with iron → Fe₃(PO₄)₂ (**vivianite**)

It should be re-solubilized to become accessible for following chemical transformations

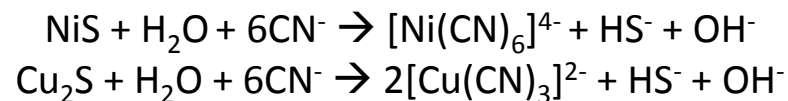
Wikimedia, Carles Millan

HCN – the crucial reactive intermediate – burning of carbon-rich chondrite meteorites into redox-neutral atmosphere containing N₂ and water



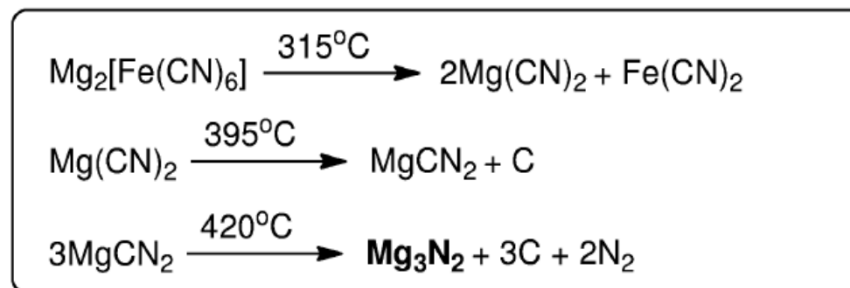
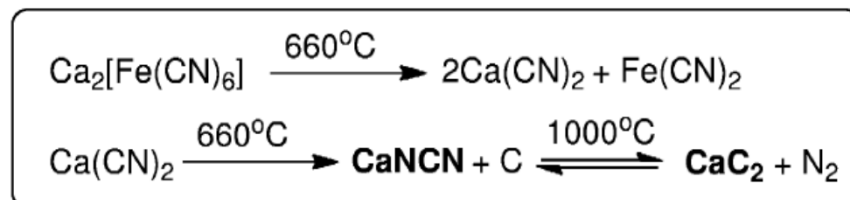
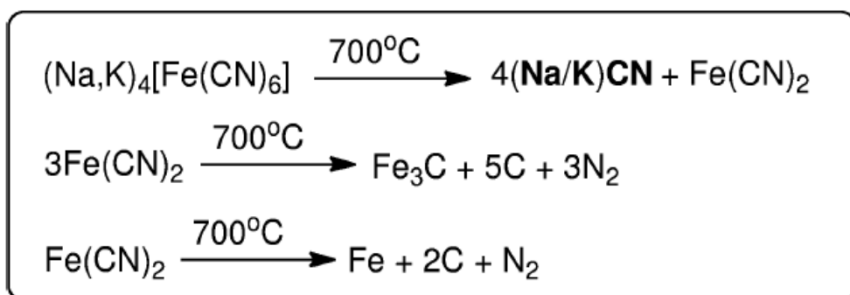
Two important functions: solubilization of phosphates and concentration of atmospheric HCN deposited as salts of mono- and divalent cations (Na, K, Mg, Ca)

Similar reactions take place with insoluble copper and nickel sulfides deposited by iron-nickel meteorite impacts (same occurrence as schreibersite, rich mining sources of these metals until today)



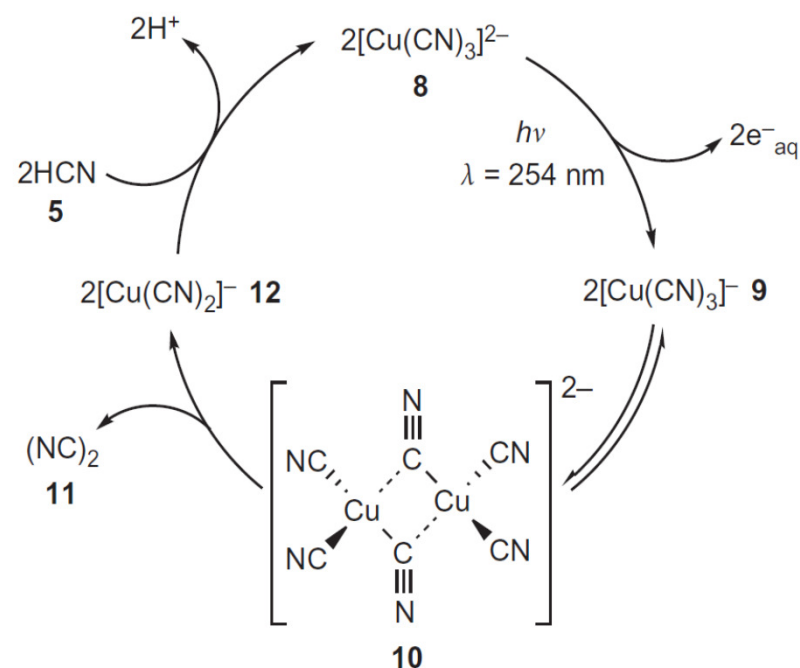
The origin of small reactive intermediates

Thermal decomposition of cyanoferrates (volcanic):

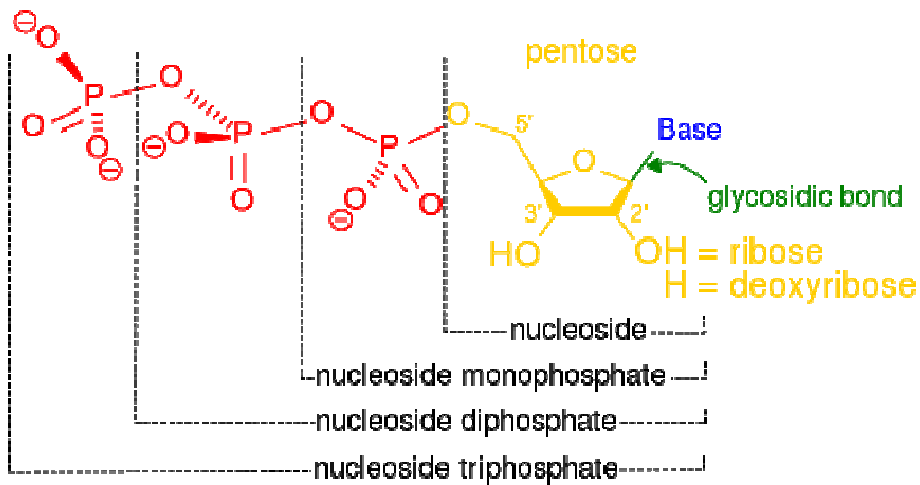
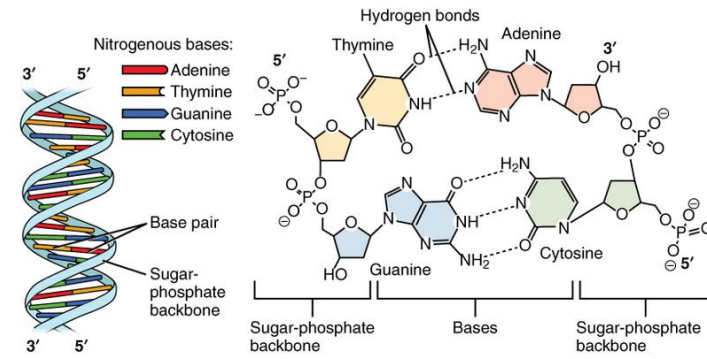
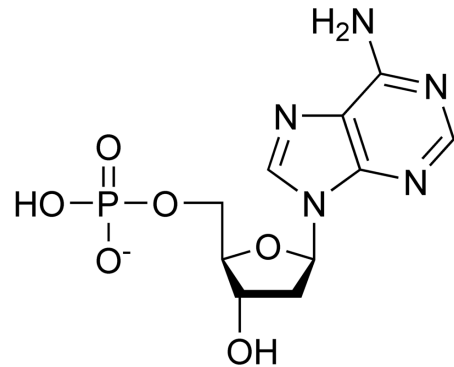


Action of water (buffered to neutral or slightly acidic) on that mixture produced concentrated HCN solution + cyanamide (from CaNCN) + acetylene (from CaC₂) + ammonia (from Mg₃N₂)

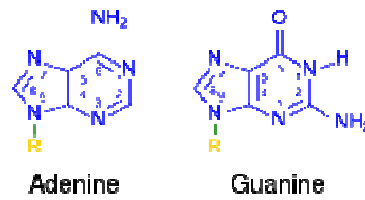
$\text{Cu}_2\text{S} + \text{H}_2\text{O} + 6\text{CN}^- \rightarrow 2[\text{Cu}(\text{CN})_3]^{2-} + \text{HS}^- + \text{OH}^-$
 cyanocuprates and HS⁻ are delivered by this process
 Photoredox cycle based on cyanocuprates may convert HCN into cyanogen



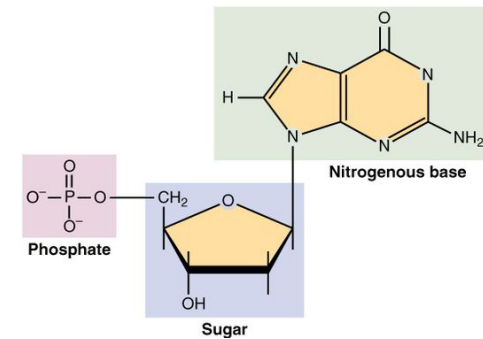
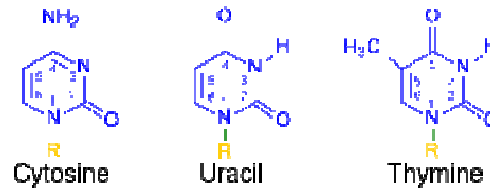
Nucleotides - components



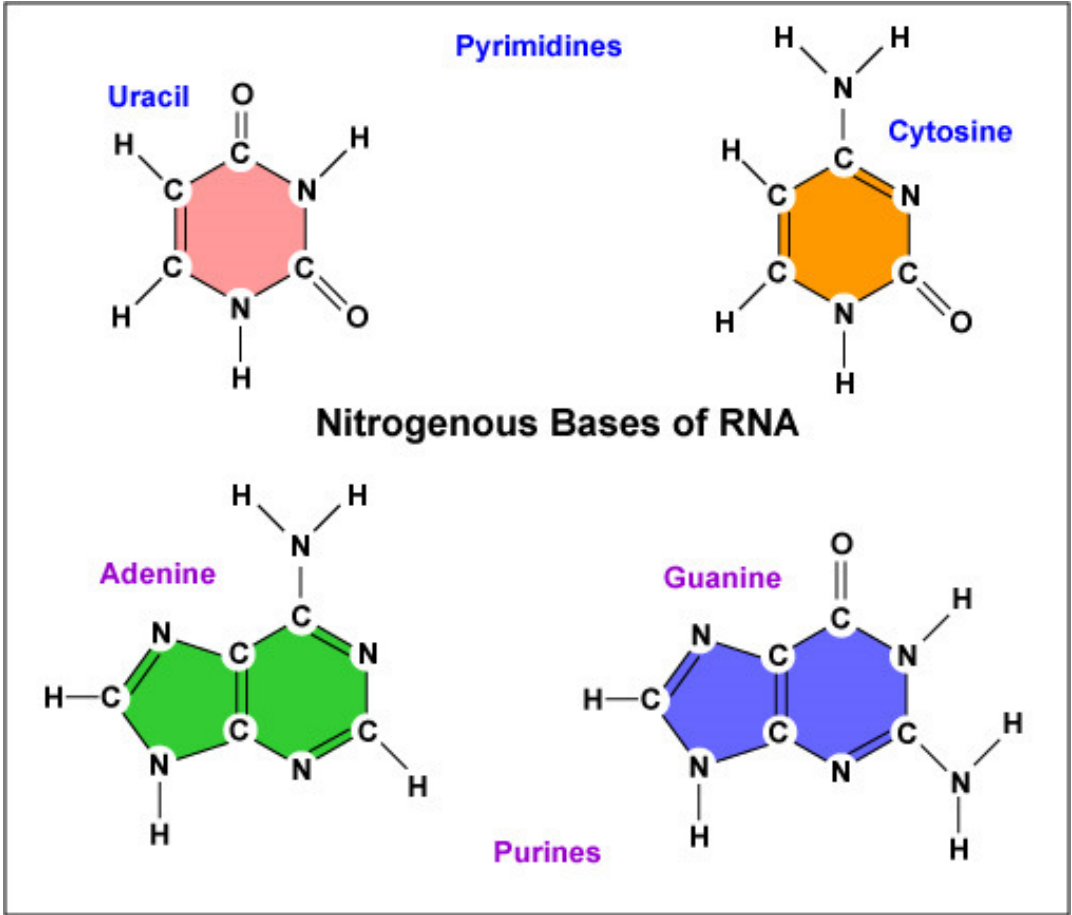
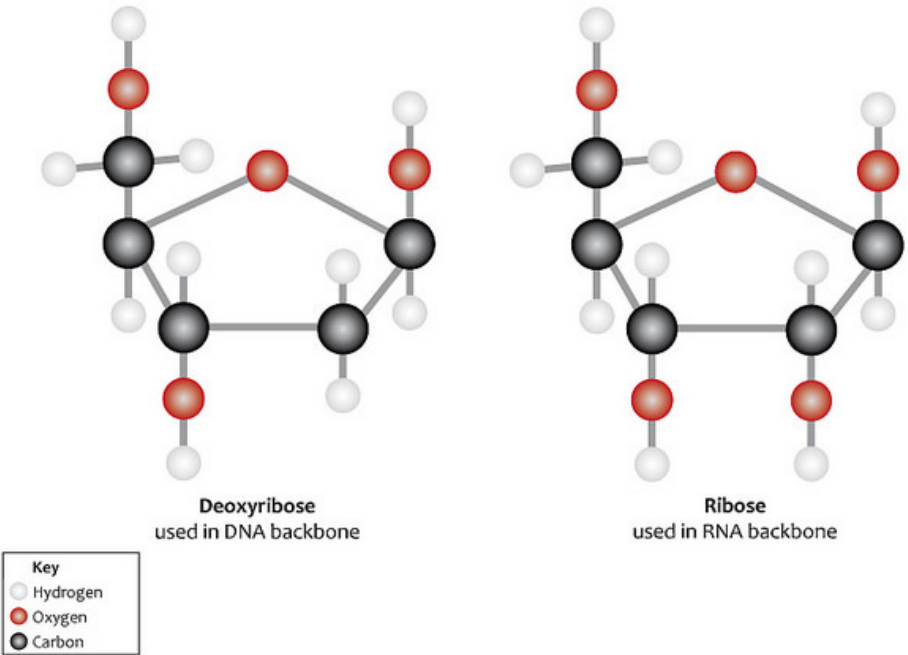
Purines



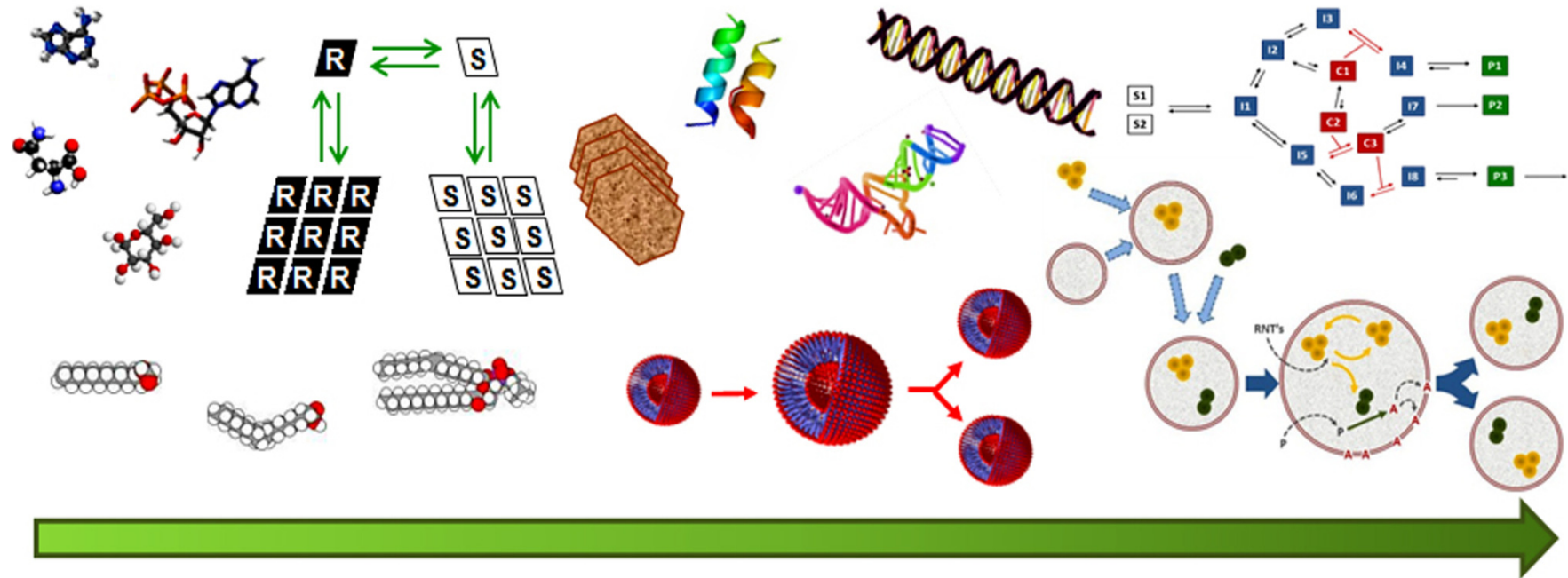
Pyrimidines



Nucleotides - nucleobases + sugars



Summary



Increasing complexity from molecules to systems

Summary

